Innovare Academic Sciences

International Journal of Pharmacy and Pharmaceutical Sciences

ISSN- 0975-1491 Vol 6, Issue 6, 2014

Original Article

PHARMACOPHORE MODELING AND QSAR STUDY OF THIENO [3, 2 - b] PYRIMIDINE ANALOGS AS VEGFR-2 INHIBITORS

PRABHU K[1], MANOJ KUMAR M[3], GOPALAKRISHNAN VK[1, 2, *]

[1] Department of Bioinformatics, Karpagam University, Coimbatore, Tamil Nadu, India 641021. [2]Department of Biochemistry, Karpagam University, Coimbatore, Tamil Nadu, India 641021. 3 Department of Biotechnology, AcharyaNagarjuna University, Guntur, Andhra Pradesh, India 522510. Email: vkgopalakrishnan@gmail.com

Received: 08 Apr 2014 Revised and Accepted: 06 May 2014

ABSTRACT

Objective: Vascular endothelial growth factor (VEGF) and its receptor tyrosine kinase VEGFR-2 are critical regulators for the activation of angiogenesis and tumor progression. Thus the VEGFR-2 inhibition represents an attractive target for drug discovery in most of the cancers. To know the structural requirements that will lead to enhanced inhibitory activities, the 3D-QSAR (quantitative structure-activity relationship) studies were performed on series of thieno [3, 2 - b] pyrimidine molecules which are having good experimental inhibitory activity.

Methods: The pharmacophore modeling analysis were performed on a series of thieno [3, 2 - b] pyrimidine analogs as inhibitors of VEGFR-2 with PHASE module of Schrödinger.

Results: The analysis showed an excellent correlation of determination value (R^2 = 0.9429) along with good statistical significance as shown by the high variance ratio (F = 78.5). The AAHRR192 model also exhibited good predictive power confirmed by the high value of the cross validated correlation of determination (Q^2 = 0.7873). The QSAR model suggests that hydrophobic character is important for the VEGFR-2 inhibitory activity, exhibited by these compounds and inclusion of hydrophobic substituent will enhance the VEGFR-2 inhibition. In addition to the hydrophobic character, electron withdrawing groups and H-bond donating groups positively contribute to the VEGFR-2 inhibition.

Conclusion: The results provide insights that will aid the optimization of these classes of VEGFR-2 inhibitors for better activity, and may prove helpful for further lead optimization, virtual screening, molecular docking and molecular dynamics (protein-ligand complex) studies.

Keywords: VEGFR-2, Pharmacophore modeling, QSAR.

INTRODUCTION

The process of new blood vessel formation from pre-existing vascular networks by capillary sprouting is called angiogenesis [1] and plays an important role in cancer [2]. It is mediated by both positive and negative factors, for which the complete physiological pathway is unknown [3]. The VEGF family is differentiated from other angiogenic super families by the mostly non-redundant roles of its members. The VEGF proteins are produced in ischemic tissues, to stipulate vessel growth, during some abnormality in vessels and if there is any undesired leakage [4].There are various tyrosine kinase inhibitors involved in tumor angiogenesis like VEGFR-2, Flt1/VEGFR-1, VEGFR-3, or PDGFR [5].

The important pathway is mediated by the vascular endothelial growth factor (VEGF) and its related cell membrane component tyrosine kinase receptor VEGFR-2 [6]. The deregulation of VEGF and VEGFR-2 leads to different pathological conditions [7]. Several studies showed the expression of VEGFR-1 and VEGFR-2 on tumor cells undergoing auto-phosphorylation, triggering signaling pathways leading to endothelial cell proliferation and subsequent angiogenesis [8, 9, 10]. The small inhibitors block the signaling pathway by competing with ATP for its binding site of the VEGFR-2 [11]. The inhibition of VEGFR-2 is an attractive strategy in the treatment of cancer [12].

Quantitative structural activity relationship (QSAR) method, is one of the most powerful and quantitative method to predict the biological activity and/or toxicity of chemicals [13]. Pharmacophore modeling is helpful to understand the protein-ligand interactions and the theoretically modeled compound [14]. It will provide wide information on molecular recognition mechanism and how to improve the biological function of a receptor or ligand. This study attempts to develop a pharmacophore model for a set of 28 VEGFR-2 inhibitors belonging to thieno [3, 2 b] pyrimidine [15] using the PHASE module of Schrödinger [16, 17].

MATERIALS AND METHODS

Ligand dataset preparation

A set of 28 thieno [3, 2 - b] pyrimidine based analogs [15] (shown in Table 1) with well-defined VEGFR-2 inhibitory activity was drawn using Maestro [18] and further used for the pharmacophore modeling and QSAR analysis. The half minimal inhibitory concentrations (IC_{50}) of the above molecules were converted into pIC_{50} [pIC_{50} = log (1 / IC_{50}), provided the unit is same] [15]. These values are used as dependent variable within the QSAR calculations. The datasets were sub categorized into three major groups based on the main chemical structure.

Pharmacophore modeling

The pharmacophore models were generated using the PHASE [19] module of Schrödinger software. The accurate calculation of 3D descriptors is performed when the compound is at appropriate conformation (lowest energy). The semi-empirical OPLS_2005 force field was implemented for energy minimization and generating conformers. For pharmacophore generation and validation, and QSAR model; the ligand molecules have been segregated into a training and test set to maintain the structural activity diversity.

In Schrödinger package, the LigPrep [20] is used to clean the selected structures, attach missing hydrogen atoms, convert 2D structures to 3D structures, create stereoisomers and neutralizes charged structures or choose the most probable ionization state at the defined pH ranging 7.0 ± 2.0 using ionizer method. It additionally permits the import of 3D structures prepared outside its own workflow. As a result of one doesn't typically recognize the structure that a given molecule can adopt if and once it binds to a target macromolecule, it's customary to represent every molecule as a series of 3D structures that represent the thermally accessible conformational states. The PHASE provides two intrinsic approaches, each of them use the macro model conformational

program for the need of pharmacophore model development. In order to increase the possibility of finding the foremost active conformer near the true structure, all possible conformers were produced to consider a range of conformations. The ligands were segregated as active and inactive based on appropriate activity threshold value. The threshold value for active ligand was 1.5 and for inactive ligand was 1.0. The activity threshold value was determined on the basis of ligand dataset activity distribution ranging between 0.227 and 3.000. Accordingly the active ligands were selected to derive a collection of appropriate pharmacophores. Those final ligands were used for generating common pharmacophore and QSAR model building.

Table 1: Chemical structures of VEGFR-2 inhibitors

Compound Number	General Structure	R^1	R^2	VEGFR-2 IC_{50} (nM)
1	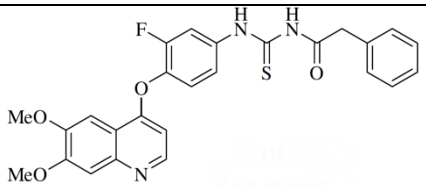	-	-	32
1a	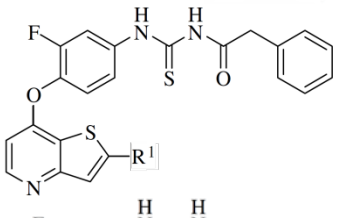	H	-	1134
1b		CH(OH)Me	-	561
1c		SMe	-	346
1d		-CO-(2-Furyl)	-	127
1e		CO_2Me	-	90
2a	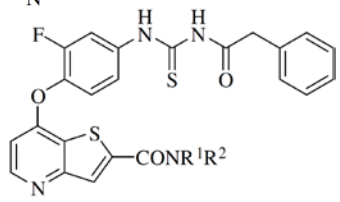	H	H	129
2b		H	Me	133
2c		Me	Me	19
2d		Et	Et	386
2e		N-Morpholine	-	289
2f		N-Pyrrolidine	-	9
2g		N-(4-Methylpiperazine)	-	344
3a	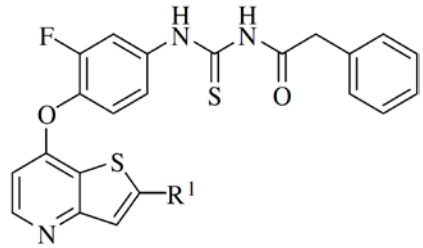	1-Methyl-1H-imidazol-4-yl	-	10
3b		1-Ethyl-1H-imidazol-4-yl	-	11
3c		1-Methyl-1H-imidazol-2-yl	-	10
3d		1-Ethyl-1H-imidazol-2-yl	-	25
3e		1-Methyl-1H-pyrazol-4-yl	-	25
3f		1-Methyl-1H-1,2,4-triazol-5-yl	-	28
3g		Thiazol-2-yl	-	17
3h		Pyridine-2-y	-	17
3i		Pyridine-3-yl	-	113
3j		Pyrimidine-2-yl	-	94
3k		1,3,4-Thiadiazol-2-yl	-	145
3l		Thiophen-2-y	-	32
3m		1-Methyl-1H-pyrrol-2-yl	-	31
3n		Furan-3-yl	-	593
3o		Pyrimidine-5-yl	-	175

Creation of pharmacophore sites

The chemical features of all ligands were outlined by six pharmacophoric features: H-bond acceptor (A), H-bond donor (D), hydrophobic group (H), negatively charged group (N), positively charged group (P), and aromatic ring (R). An active analog approach was used to identify common pharmacophore hypotheses (CPHs), in which common pharmacophores were collected from the conformations of the active set ligands using a tree-based partitioning technique that groups together similar pharmacophores according to their inter-site distances. These features follow a set of SMARTS pattern.

Identifying common pharmacophores

The pharmacophores having identical features are clustered together with their similar spatial arrangements. A common pharmacophore is derived when a given group is found to contain at least one pharmacophore from each ligand. Those common pharmacophores are identified from a set of variants, which set of feature types that define a possible pharmacophore. Based on the common features among the ligands, the total number of points is to be selected for further studies. A best pharmacophore hypothesis AAHRR192 was selected after carefully examining the scores and alignment of active ligands to the hypothesis. The generated 3D pharmacophore hypothesis comprises of the following features: Two hydrogen bond acceptors (A), two aromatic rings (R) and one hydrophobic group (H). Subsequently the derived common pharmacophore hypothesis was scored for matching the in-actives just like the calculation of survival score of the actives.

Scoring pharmacophores with respect to active and inactive ligands

The best pharmacophore provides a hypothesis to explain how the active molecules bind to the receptor. The scoring and ranking were performed on the resulted pharmacophore. The scoring was done to spot the most effective candidate hypothesis that provided associate overall ranking of all the hypotheses. The alignment of site points and vectors, selectivity, volume overlap, relative conformational energy, number of ligands matched, and activity are the major components of scoring algorithm. The quality of alignment is measured in three ways: the alignment score, the vector score and the volume score. The following equation has been used for the final survival scoring process.

$S = W_{site}\ S_{site} + W_{vec}\ S_{vec} + W_{vol}\ S_{vol} + W_{sel}\ S_{sel} + W^{m}_{rew} - W\ \Delta E + W_{act}\ A$

Where W's indicate weights and S's indicate scores. Additionally, an adjusted survival score is derived using the following equation using a weight of 1.0 for the inactive scores.

$S_{adj} = S_{actives} - W_{inactives}\ S_{inactives}$

Building 3D-QSAR models

The QSAR modeling was performed using the selected hypothesis; and by separating the ligand dataset randomly into 70% training set compounds and 30% test set compounds [21]. There are two choices for alignment of 3D structure of molecules in PHASE: the pharmacophore based alignment and atom based alignment. In this study, atom based QSAR model is considered, which is more useful and appropriate in elucidating the structure-activity relationship. A molecule is managed as a setoff overlapping van der Waal's spheres. Each atom (and hence each sphere) is placed into one of six categories according to a simple set of rules: hydrogens attached to polar atoms are classified as hydrogen bond donors (D); atoms with an explicit negative ionic charge are classified as negative ionic (N); carbons, halogens, and C-H hydrogens are classified as hydrophobic/non-polar (H); atoms with an explicit positive ionic charge are classified as positive ionic (P); non-ionic nitrogen and oxygen are classified as electron-withdrawing (W); and all other types of atoms are classified as miscellaneous (X).

For the aim of QSAR development, van der Waal's models of the aligned training set molecules were placed in a very regular grid of cubes, with every cube assigned zero or additional 'bits' to account for various sorts of atoms within the training set that occupy the cube. This illustration provides rise to binary-valued occupation patterns that may be used as independent variables to make partial least-squares (PLS) QSAR models. Atom-based QSAR models were generated for the chosen hypothesis exploitation the 24-member training set employing a grid spacing of 1.0 Å. The 10 test set compounds were used to validate the most effective QSAR model. A single model with good statistic was obtained for the dataset using the following equations.

$$r^2 = 1 - [\sum(Y_{pred} - Y_{obs})^2 / \sum(Y_{obs} - Y_{mean})^2]$$

Where, Y_{pred}, Y_{obs} and Y_{mean} indicate the predicted, observed and mean biological activity values. The value generated from is the predicted residual sum of squares (PRESS). The correlation coefficient of determination for test set compounds is also calculated using the same above equation.

RESULTS AND DISCUSSION

The aim of the study was to produce 3D pharmacophore and to elucidate the structure features of VEGFR-2 inhibitors using the ligand based drug design approach. It is also crucial to understand the mode of binding and interaction which are essential for biological activity. The PHASE module of Schrödinger suite has been used for pharmacophore modeling and QSAR studies. The binding nature of ligand inside the active site of the receptor has been projected by the hypothesis generated by PHASE. In 3D-QSAR model, the identification of molecular activity has been performed by using the conformation structure identified by hypothesis.

The 5 compounds having activity >= 2, in pharmacophore model generation, were used against the VEGFR-2 as active as they have important binding sites to the receptor. The optimum variant list was generated with minimum and maximum of five sites. Using the above condition, six pharmacophore models were produced with different set of variants and all the models were utilized for common pharmacophore model generation. The models which were showing best alignments with active compounds were picked by calculating the survival score. The survival score algorithm identifies the superior candidate hypothesis from the generated models and generates an overall ranking of the entire hypothesis. It includes various components from the alignment of site points and vectors, relative conformational energy, selectivity, number of ligands matched, volume overlap, and activity.

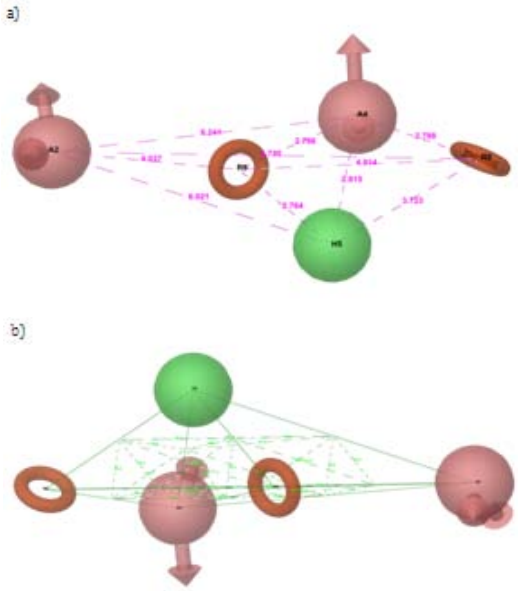

Fig. 1: Geometry of the pharmacophore (a) CPH with distances (b) CPH with angles

Acceptor (A) - Light red sphere centered on the atom with the lone pair, with arrows pointing in the direction of the lone pairs

Donor (D) - Light blue sphere centered on the H atom, with an arrow pointing in the direction of the potential H-bond

Hydrophobic (H) - Green sphere

Negative (N) - Red sphere

Positive (P) - Blue sphere

Aromatic Ring (R) - Orange torus in the plane of the ring

However, the pharmacophore should also differentiate between the active (high active) and inactive (low active) molecules. It is also crucial to understand the prevention of inactive ligands from binding. To justify it, the pharmacophore models were mapped to inactive compounds and scored. The hypothesis could be wrong if the inactive ligands score well because it does not differentiate between active and inactive ligands. Hence, adjusted survival score was calculated by subtracting the inactive score from survival score of those pharmacophores. Ultimately, model AAHRR192, which was having maximum adjusted survival score and lowest relative conformational energy, has been selected for generating atom based alignment of VEGFR-2 inhibitors. The 3D QSAR hypothesis has been generated using 24 training set compounds and validated using 10 test set compounds. Those compounds cover wide range of VEGFR-2 inhibitory activity as enumerated in table 2. A four PLS factor model with good statistics and predictive ability were derived from the dataset. The model expressed ~73% variance exhibited by thieno [3, 2 - b] pyrimidine derivatives and illustrate the best fitting points on the regression line for the observed and PHASE predicted activity. The geometric orientation of features in hypothesis has been illustrated in figures 1a and 1b. A 3D-QSAR analysis was performed on the series of thieno [3, 2 - b] pyrimidine derivatives to visualize the effect of spatial arrangement of structural features on their VEGFR-2 inhibitors, which are diagrammatically represented in figures 2a, 2b, 2c and 2d. The high value of F (78.5) and low value of p, an indication of high degree of confidence, indicates a statistically significant model. This is also supported by the small values of RMSE (0.2084) and standard deviation (0.1933). The table 3 summarizes the partial least squares analysis results of the best common pharmacophore hypothesis AAHRR192. The figure 3a also illustrates that the hypothesis generated using the random training set is more accurate. In contrast, the plot is scattered in figure 3b for test set

compounds. In figure 3c, the fitness score for both training and test compounds were colored using different colors.

Table 2: Alignments for the best common pharmacophore hypothesis

Ligand Name	Actual pIC_{50}	PLS Factors	Predicted pIC_{50}	Fitness	Ligand Name	Actual pIC_{50}	PLS Factors	Predicted pIC_{50}	Fitness
1*	1.50	1	1.60	1.73	3b*	1.96	1	1.14	0.80
		2	1.38				2	1.51	
		3	1.45				3	1.61	
		4	1.39				4	1.51	
1a*	-0.06	1	0.24	1.58	3b	1.96	1	1.83	1.71
		2	0.03				2	1.72	
		3	-0.29				3	2.34	
		4	-0.23				4	2.62	
1b*	0.25	1	0.08	1.36	3c*	2.00	1	1.61	0.79
		2	0.04				2	1.95	
		3	0.30				3	2.33	
		4	0.40				4	2.12	
1b*	0.25	1	0.44	1.22	3c*	2.00	1	1.78	2.06
		2	0.38				2	1.96	
		3	0.17				3	1.75	
		4	0.14				4	2.05	
1c*	0.46	1	0.26	1.14	3d*	1.60	1	1.61	1.45
		2	0.24				2	1.76	
		3	0.56				3	1.54	
		4	0.66				4	1.56	
1d*	0.90	1	0.90	0.80	3d*	1.60	1	1.74	1.68
		2	1.16				2	1.52	
		3	0.98				3	1.69	
		4	0.74				4	1.66	
1e*	1.05	1	1.63	1.69	3e*	1.60	1	1.76	2.07
		2	1.34				2	1.91	
		3	1.29				3	1.60	
		4	1.10				4	1.82	
2a*	0.89	1	1.59	1.69	3f*	1.55	1	1.69	1.69
		2	1.30				2	1.44	
		3	1.19				3	1.57	
		4	0.96				4	1.50	
2b*	0.88	1	0.88	0.79	3g	1.77	1	1.51	1.45
		2	0.86				2	1.64	
		3	0.94				3	1.46	
		4	0.89				4	1.46	
2c*	1.72	1	1.67	3.00	3h*	1.77	1	1.77	2.08
		2	1.63				2	1.93	
		3	1.63				3	1.65	
		4	1.81				4	1.89	
2d	0.41	1	1.50	1.44	3i	0.95	1	1.74	2.08
		2	1.63				2	1.90	
		3	1.45				3	1.64	
		4	1.44				4	1.88	
2e*	0.54	1	0.26	1.33	3j*	1.03	1	1.66	1.66
		2	0.34				2	1.37	
		3	0.60				3	1.36	
		4	0.71				4	1.18	
2f*	2.05	1	1.82	1.41	3k*	0.84	1	1.07	0.80
		2	2.05				2	1.38	
		3	2.12				3	1.28	
		4	2.02				4	1.02	
2g*	0.46	1	0.80	0.85	3l	1.50	1	1.66	1.69
		2	0.63				2	1.45	
		3	0.16				3	1.63	
		4	0.24				4	1.62	
2g	0.46	1	0.95	0.80	3m	1.51	1	1.67	1.67
		2	1.20				2	1.43	
		3	1.08				3	1.55	
		4	0.88				4	1.49	
3a	3.00	1	1.76	2.07	3n	0.23	1	1.69	1.68
		2	1.92				2	1.48	
		3	1.63				3	1.71	
		4	1.87				4	1.73	
3a*	3.00	1	1.84	1.71	3o	0.76	1	0.94	0.80
		2	1.73				2	1.21	
		3	2.35				3	1.09	
		4	2.64				4	0.89	

* - Training set compounds. The remaining is used as test set compounds.

Table 3: Summary of partial least-squares analysis results for the best common pharmacophore hypothesis (CPH)

Hypothesis	No of Factors	SD	R^2	F	p	RMSE	Q^2	Pearson-R
AAHRR192	1	0.4275	0.6768	46.1	8.070×10^{-7}	0.5923	0.7690	0.1126
	2	0.3738	0.7642	34.0	2.585×10^{-7}	0.5924	0.7733	0.1025
	3	0.2636	0.8883	53.0	1.062×10^{-9}	0.2538	0.7989	0.0421
	4	0.1933	0.9429	78.5	1.532×10^{-11}	0.2084	0.7873	0.0699

SD - Standard deviation of the regression, R^2 - Correlation coefficient of determination, F - Variance ratio, p - Significance level of variance ratio, RMSE - Root mean square error, Q^2 - Correlation coefficient of determination of predicted activities, Pearson-R - Correlation between predicted and observed activity for the test set.

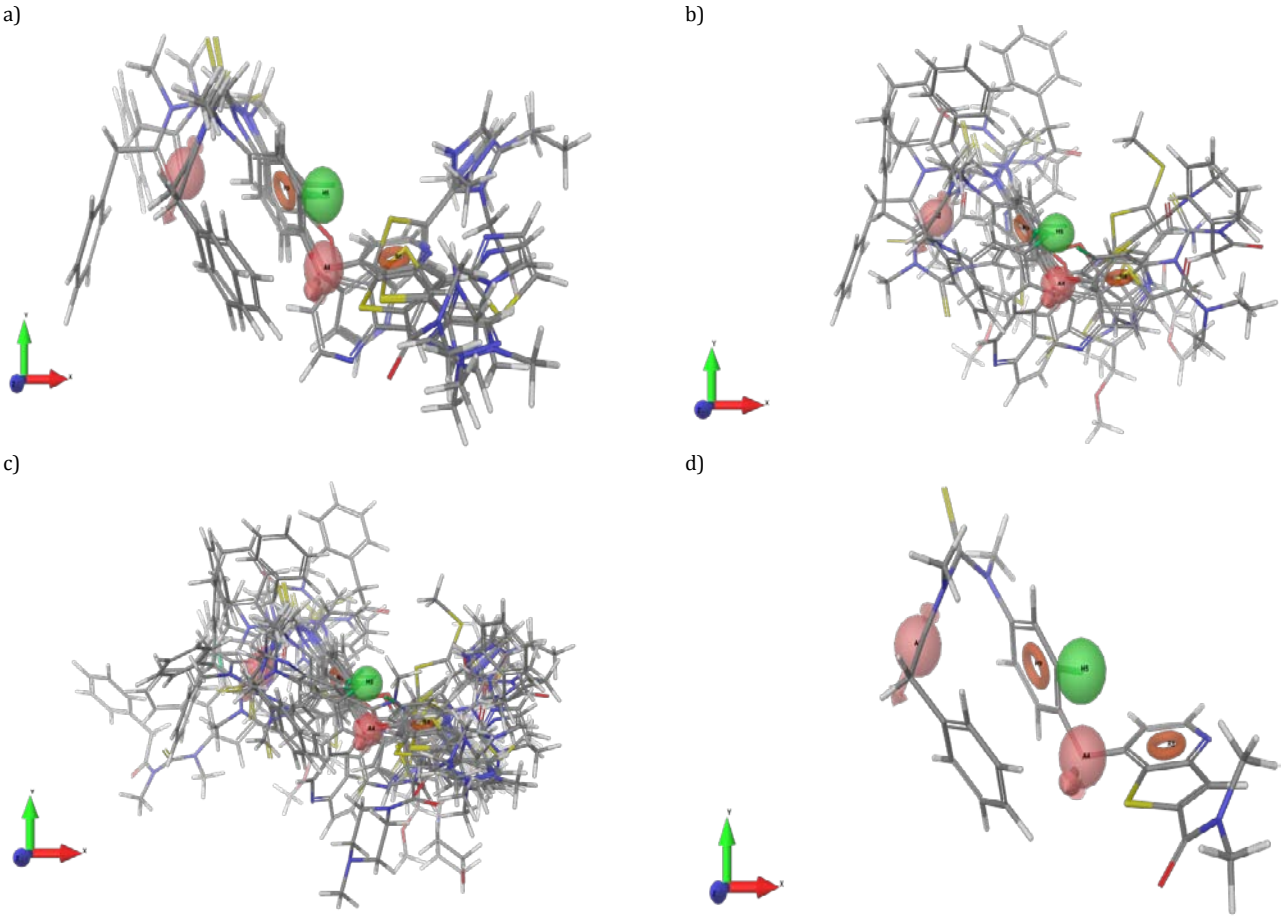

Fig. 2: Orientation of ligands on common pharmacophore hypothesis (a) CPH with most active ligands (b) CPH with most inactive ligands (c) CPH with all the ligands (d) CPH with the best ligand

As portrayed in figure 2d, among the two aromatic rings, one is associated with the main thieno [3, 2 - b] pyrimidine structure and another on benzene side chain attached to pyrimidine structure. One of the hydrogen bond acceptor group is mapped to carboxyl group on side chain attached to thieno [3, 2 - b] pyrimidine structure and the other hydrogen bond acceptor is mapped to aryl ether group. In the model, the atoms may contribute positively or negatively to the activity.

The color coded cubes in the 3D-QSAR model are according to the coefficient values. The blue is for positive coefficient or increased activity and the red if for negative coefficient or decreased activity.

The orientation of color codes, as portrayed in various figure 4 categories, helps us to identify the relevant or irrelevant functional groups at specific positions of a molecule. The blue cube regions indicate the requirement of essential feature to improve the activity and on other hand the red cubes indicate the non-essential functional groups or features.

There are more blue cubes in figure 4a because of surrounding benzene rings. The figure 4b depicts that the blue cubes presence at the A2 position indicates the good possibility of increasing the electron withdrawing effect of the molecules. Adding some suitable electron withdrawal group near that will improve the VEGFR-2 inhibition, whereas the putting some electron withdrawal group at A4 is not going to improve the receptor binding activity of inhibitors, as it is mostly surrounded by red cubes because of the aromatic rings.

The figure 4c represents the feature (sulphur in this case) of other groups. The figure 4d represents the combined effect of all the above features of the best pharmacophore model with the best fit ligand.

On contrast, the figures 4e, 4f, 4g, 4h illustrates the individual features of best pharmacophore model with the most inactive ligand. In most of the inactive ligand set contours, the red cubes are more predominant indicating that those structures were not suitable for the best pharmacophore and in turn proves that the current AAHRR192 pharmacophore model is more stable and the cross validation with test set compounds are also perfect.

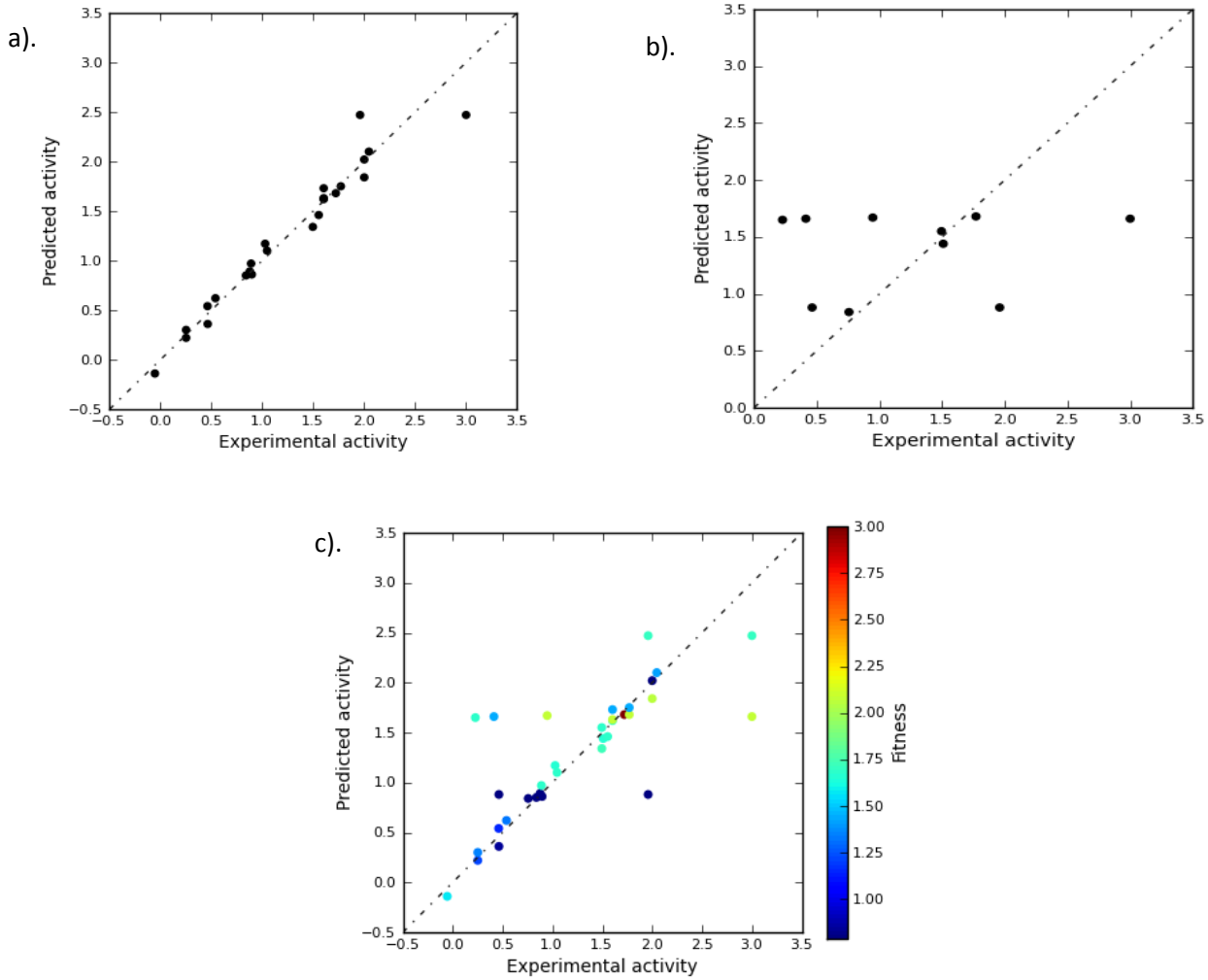

Fig. 3: Scatter plots for the predicted and experimental pIC50 values (a) Training set (b) Test set (c) Training and test set with fitness score

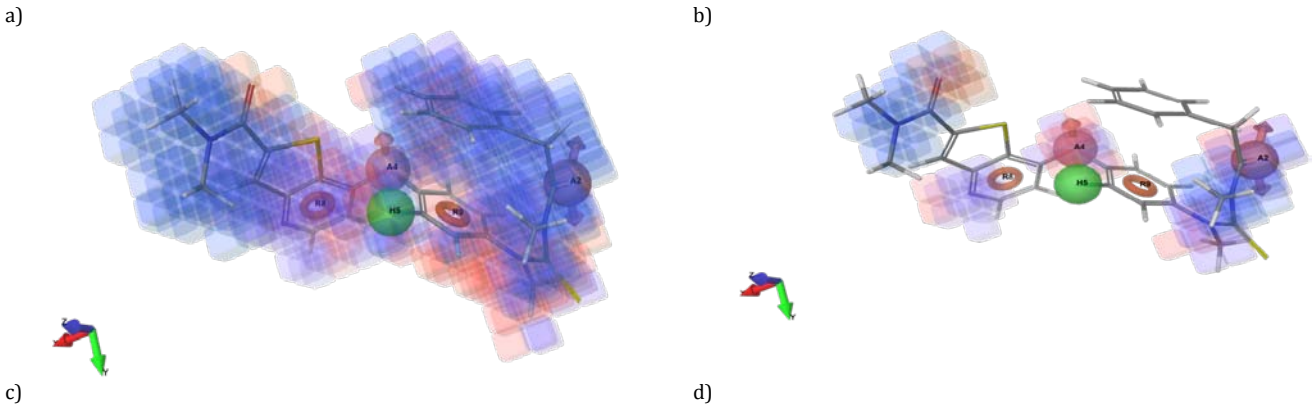

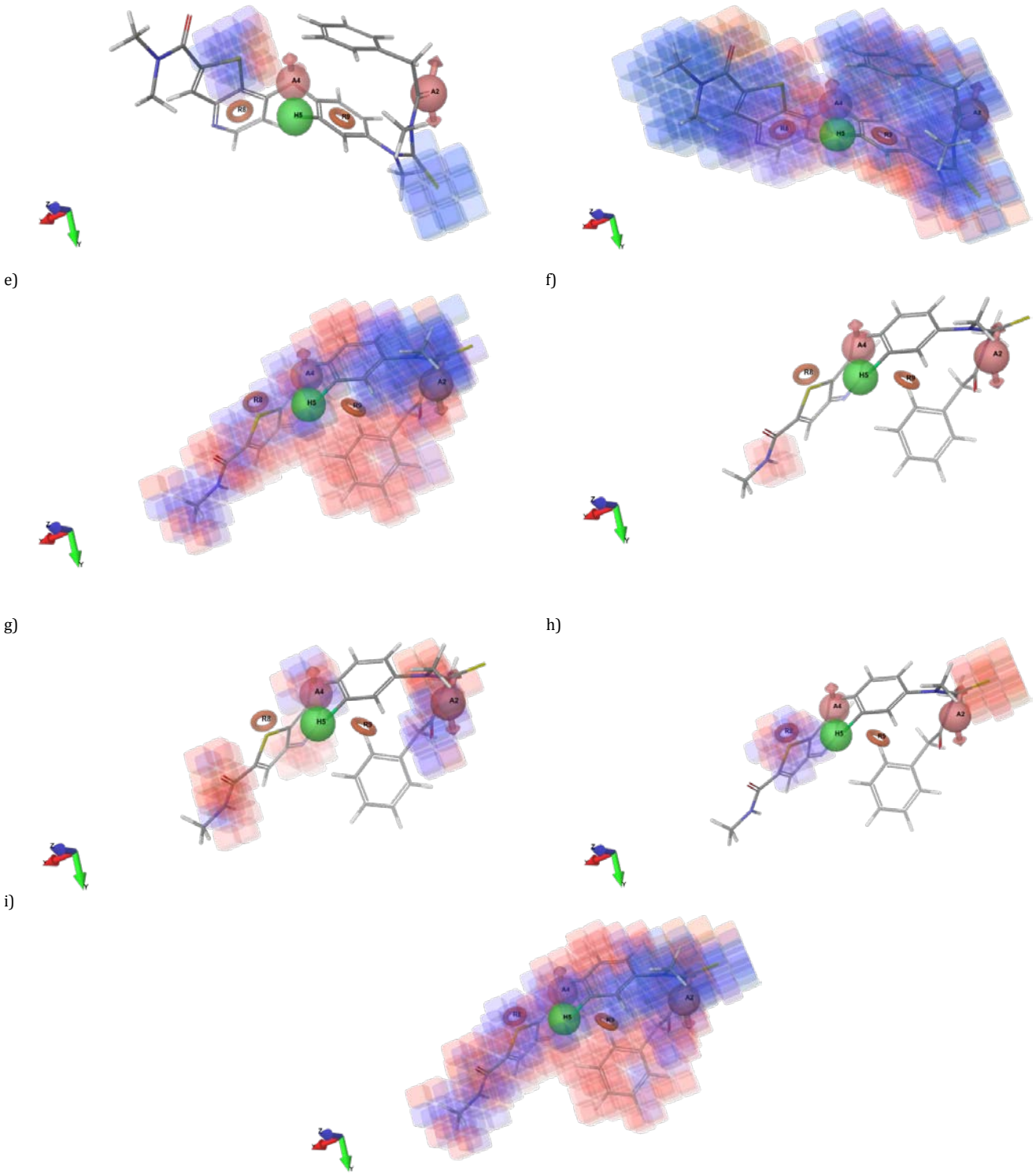

(a), (e) Hydrophobic / non-polar feature on most active and inactive ligand (b), (g) Electron-withdrawing feature on most active and inactive ligand (c), (h) Other features on most active and inactive ligand (d), (i) All features on most active and inactive ligand (f) H-bond donor feature on inactive ligand

Fig. 4: Diagrammatic representation of contours generated using the QSAR model. Blue cubes indicate favorable regions while red cubes indicate unfavorable region for the activity.

CONCLUSION

In drug designing and discovery, pharmacophore modeling is a very powerful method enabling chemists to rapidly identify the new potential drugs by revealing the structural components responsible for biological activity. With the help of pharmacophore based alignment of VEGFR-2 inhibitors, the highly predictive 3D-QSAR model using 24 training set molecules which consists of five point pharmacophore hypothesis i.e., AAHRR192 was created. The generated ligand-based pharmacophore hypothesis emphasize the critical binding features for novel thieno [3, 2 b] pyrimidine derivatives as VEGFR-2 inhibitors. This atom based 3D-QSAR model

stipulates some thoughts into the structural requirement of novel VEGFR-2 inhibitors. The identification and analysis of potential roles of specific residues within thieno [3, 2 - b] pyrimidine derivatives are also crucial for rational design of selective ligands. This study will provide us further guidance to perform virtual screening, molecular modeling, lead optimization of new potent VEGFR-2 inhibitors, and molecular dynamics of the VEGFR-2 protein and ligand complex.

ACKNOWLEDGEMENT

The authors would like to thank the Chancellor, Chief Executive Officer, Vice Chancellor, and Registrar of Karpagam University for providing facilities and encouragement; Sumathy R, Chella Perumal P for helping in preparing this manuscript; and Dr. Raghu, EO, Schrödinger for providing software support.

DECLARATION OF INTEREST

The authors report no declaration of interest.

REFERENCES

1. Folkman J, Shing Y. Angiogenesis. The Journal of biological chemistry 1992;267(16):10931-4.
2. Patan S. Vasculogenesis and angiogenesis as mechanisms of vascular network formation, growth and remodeling. Journal of neuro-oncology 2000;50(1-2):1-15.
3. Ferrara N, Kerbel RS. Angiogenesis as a therapeutic target. Nature 2005;438(7070):967-74.
4. Carmeliet P, Jain RK. Molecular mechanisms and clinical applications of angiogenesis. Nature 2011;473(7347):298-307.
5. Muthukumaran R, Sangeetha B, Amutha R, Premendu PM. Pharmacophore based 3D-QSAR modeling and free energy analysis of VEGFR-2 inhibitors. Journal of Enzyme Inhibition and Medicinal Chemistry 2013;28(6):1236-46.
6. Lemmon MA, Schlessinger J. Cell signaling by receptor tyrosine kinases. Cell 2010;141(7):1117-34.
7. Mammoto A, Connor KM, Mammoto T, Yung CW, Huh D, Aderman CM, *et al.* A mechanosensitive transcriptional mechanism that controls angiogenesis. Nature 2009;457(7233):1103-8.
8. Lee T-H, Seng S, Sekine M, Hinton C, Fu Y, Avraham HK, *et al*. Vascular endothelial growth factor mediates intracrine survival in human breast carcinoma cells through internally expressed VEGFR1/FLT1. PLoS medicine 2007;4(6):e186.
9. Silva SR, Bowen KA, Rychahou PG, Jackson LN, Weiss HL, Lee EY, *et al*. VEGFR-2 expression in carcinoid cancer cells and its role in tumor growth and metastasis. International journal of cancer 2011;128(5):1045-56.
10. Chung GG, Yoon HH, Zerkowski MP, Ghosh S, Thomas L, Harigopal M, *et al*. Vascular endothelial growth factor, FLT-1, and FLK-1 analysis in a pancreatic cancer tissue microarray. Cancer 2006;106(8):1677-84.
11. Pedro S, Raquel C, Hugo JCF, Ricardo CC, Daniela P, Isabel C, *et al*. 1-Aryl-3-[4-(thieno[2-d]pyrimidin-4-yloxy)phenyl] ureas as VEGFR-2 Tyrosine Kinase Inhibitors: and Molecular Modeling Studies. BioMed Research International 2013;3
12. Ferrara N, Hillan KJ, Gerber H-P, Novotny W. Discovery and development of bevacizumab, an anti-VEGF antibody for treating cancer. Nature reviews. Drug discovery 2004;3(5):391-400.
13. Vilar S, González-Díaz H, Santana L, Uriarte E. A network-QSAR model for prediction of genetic-component biomarkers in human colorectal cancer. Journal of theoretical biology 2009;261(3):449-58.
14. Xiao JF, Guo ZG, Guo YS, Chu FM, Sun PY. Inhibitory mode of N-phenyl-4-pyrazolo[1,5-b] pyridazin-3-ylpyrimidin-2-amine series derivatives against GSK-3: molecular docking and 3D-QSAR analyses. Protein engineering, Design & Selection. 2006; 19: 47-54.
15. Claridge S, Raeppel F, Granger M-C, Bernstein N, Saavedra O, Zhan L, *et al*. Discovery of a novel and potent series of thieno[3,2-b]pyridine-based inhibitors of c-Met and VEGFR2 tyrosine kinases. Bioorganic & medicinal chemistry letters 2008;18(9):2793-8.
16. Dixon SL, Smondyrev AM, Knoll EH, Rao SN, Shaw DE, Friesner RA. PHASE: a new engine for pharmacophore perception, 3D QSAR model development, and 3D database screening: 1. Methodology and preliminary results. Journal of computer-aided molecular design 2006;20(10-11):647-71.
17. Evans DA, Doman TN, Thorner DA, Bodkin MJ. 3D QSAR Methods: Phase and Catalyst Compared. Journal of Chemical Information and Modeling. 2007; 3: 1248-1257.
18. Maestro, version 9.3, Schrödinger, LLC, New York, NY, 2012.
19. Phase, version 3.4, Schrödinger, LLC, New York, NY, 2012.
20. LigPrep, version 2.5, Schrödinger, LLC, New York, NY, 2012.
21. Mahesh KT, Pradeep H, Rajanikant GK. Pharmacophore Generation and 3D-QSAR of Novel 2-(quinazolin-4ylamino)-[4] Benzoquinone Derivatives as VEGFR-2 Inhibitors. Letters in Drug Design and Discovery 2012;1.